Tunnelling and Underground Space Technology 131 (2023) 104829

Contents lists available at ScienceDirect

Tunnelling and Underground Space Technology incorporating Trenchless Technology Research

journal homepage: www.elsevier.com/locate/tust

Experimental analysis of the effect of the ramp slopes on the maximum exceedance temperature in a branched tunnel fire

Jiaxin Li [a,c], Yanfeng Li [a,*], Junmei Li [a], Hua Zhong [b,*], Jianlong Zhao [a], Desheng Xu [a]

[a] Beijing Key Laboratory of Green Built Environment and Energy Efficient Technology, Beijing University of Technology Beijing, China
[b] School of Architecture, Design and Built Environment, Nottingham Trent University, Nottingham NG1 4FQ, United Kingdom
[c] School of Civil and Environmental Engineering, Nanyang Technological University, Singapore

ARTICLE INFO

Keywords:
Maximum exceedance temperature
Ramp slopes
Branched tunnels
Longitudinal ventilation

ABSTRACT

This research aims to establish a series of small-scale experiments to analyze the effect of ramp slopes on the temperature distribution of Liquefied Petroleum Gas (LPG) fire in a model branched tunnel under longitudinal ventilation. The heat release rate under experimental conditions reached 2.57 kW to 7.70 kW and five ramp slopes of 0 %, 3 %, 5 %, 7 % and 9 % were conducted. For a specific given bifurcation angle, the maximum exceedance temperature of the fire in the expanding region before the bifurcation angle is measured and analysed. Results show that the maximum exceedance temperature in the main tunnel increases as the ramp slope decreases, which is mainly because the stack effect enhances the entrainment of the air and accelerates the smoke flow. Furthermore, the modified model of the maximum exceedance temperature, which could consider the influence of ramp slope for a branch tunnel fire is established according to the experimental results. The predicted results agree well with those of the experimental study for the main tunnel. The results could provide a reference and contribute to the knowledge of smoke extraction strategies designed for branched tunnels.

1. Introduction

In modern cities, road tunnels play a significant role in social development and people's daily lives, and the probability of a tunnel fire is increasing with the increasing traffic volume. Because of the serious consequences of a tunnel fire, the tunnel fire characteristics have received extensive attention, including heat release rate (Ingason and Lönnermark, 2005; Tomar and Khurana, 2019), fire plume (Zukoski et al., 1981; Heskestad, 1983; McCaffrey, 1979), temperature distribution (Alpert, 1972; Li et al., 2011; Zhou et al., 2021), smoke movement (Tanaka et al., 2021; Zhang et al., 2021a, 2021b, 2021c). Taking the tunnel construction into consideration, Zhang et al., (2021a, 2021b, 2021c) carried out sophisticated analyses to derive the influence of tunnel cross-section, and tunnel slope (Chow et al., 2015) on the tunnel fire characteristics. The three main reasons that the vehicle self-ignition, vehicle collision, and over-turning bring about the tunnel fire lead the fire location of a tunnel fire accident to be random (Wang et al., 2016). The effects of the blockage ratio (Wang et al., 2021; Zhang et al., 2021a, 2021b, 2021c), the transverse fire location (Ji et al., 2012) and the longitudinal fire location (Kong et al., 2021) on the tunnel fire characteristics had been analyzed. Natural ventilation systems and longitudinal ventilation systems are two effective methods of smoke control in tunnels for reducing casualties and economic losses. The stack effect induced by the density difference in vertical height had been investigated in an inclined tunnel with natural ventilation (Zhang et al., 2021a, 2021b, 2021c). The critical velocity (Gannouni, 2022), the minimum longitudinal ventilation required to prevent smoke backflow, is a significant parameter for the design of a tunnel exhaust system for fire smoke. However, most previous literature paid close attention to the fire characteristics of ordinary single tunnels. Nowadays, branched tunnels and urban traffic link tunnels (UTLTs) are prevailing with the continuous development of the urban economy and the increasing traffic pressure (Li et al., 2022). The complicated structure of split tunnels makes them different in the smoke movement and the maximum exceedance temperature in fire scenarios. Thus, it is necessary to pay significant attention to research on the effect of the ramp slope on the smoke movement and the maximum exceedance temperature in a branched tunnel fire

Considering the research on fire characteristics in ordinary single tunnels, Huang et al. (2019) carried out a series of small-scale tests to analyze the influence of bifurcation angles on the smoke temperature distribution in fire scenarios of a horizontal branched tunnel. A predicted equation of the maximum exceedance temperature was proposed,

* Corresponding authors.
E-mail addresses: liyanfeng@bjut.edu.cn (Y. Li), hua.zhong@ntu.ac.uk (H. Zhong).

https://doi.org/10.1016/j.tust.2022.104829
Received 29 May 2022; Received in revised form 16 October 2022; Accepted 24 October 2022
Available online 4 November 2022

Nomenclature

Abbreviation

Q	Heat release rate (kW)
Q*	non-dimensional heat release rate with effective tunnel height
T∞	ambient temperature (K)
V'	non-dimensional ambient velocity
ΔT_{max}	Maximum temperature excess (K)
g	gravitational acceleration (m/s^2)
Z_0	Virtual origin height (m)
l	tunnel length (m)
D	fire source diameter (m)
c_p	The specific heat capacity of air (kJ/kg·K)
Z_0	Virtual origin height (m)
u_0	ambient velocity (m/s)

Greek and other symbols

θ	Ramp slope (%)
ρ∞	ambient density (kg/m^3)
δ,ψ	coefficients about the bifurcated angle
ξ,φ	coefficients about the bifurcated angle
α_θ	coefficients about the bifurcated angle

Subscripts

f	full scale
m	model scale

which could be described as the following equations:

$$\frac{\Delta T_{\max}}{T_\infty} = \begin{cases} 2.5(Q^*)^{2/5}, V' \leqslant 0.19 \\ \delta\left(1.71V^{-5/6}a(Q^*)^{2/3}\right)^{\psi}, V' > 0.19 \end{cases} \quad (1)$$

$$Q^* = \frac{Q}{T_\infty c_p \rho_\infty \sqrt{g(0.95H - Z_0)^5}} \quad (2)$$

$$Z_0 = 0.083Q^{2/5} - 1.02D \quad (3)$$

$$V' = u_0\left(\frac{Q}{D/2c_p\rho_\infty T_\infty}\right)^{-1/3} \quad (4)$$

$$\delta = \left(1.332 - 3.548\sin\theta + 9.889\sin^2\theta\right) \quad (5)$$

$$\psi = \left(0.979 - 4.464\sin\theta + 13.833\sin^2\theta\right) \quad (6)$$

where ΔT_{max} is the maximum exceedance temperature, c_p is the specific heat capacity in kJ/(kg•K), Q^* is the non-dimensional heat release rate, V' is non-dimensional velocity, Q is the heat release rate in kW, H is the tunnel height in m, T_∞ is ambient temperature, ρ_∞ is the ambient air density in kg/m^3, Z_0 is the virtual origin height in m, u_0 is longitudinal ventilation velocity in m/s, D is the characteristic diameter of the fire source in m, δ and ψ are coefficients about the bifurcated angle, θ is the bifurcated angle.

Huang et al. (2020, 2021, 2022) established two models of the critical longitudinal ventilation velocity and the smoke back-layering length under longitudinal ventilation, and investigated the effect of longitudinal ventilation and split angle on the longitudinal temperature decay in a branched tunnel by conducting theoretical analysis and experiments. Chen et al. (2020a, 2020b) indicated that the maximum exceedance temperature would rise significantly when the fire source was located at the bifurcation area. Lei et al. (2021) and Li et al. (2021a, 2021b, 2021c) investigated the effect of the fire locations on the maximum exceedance temperature through experimental and theoretical studies in branched tunnel fires. Lu et al. (2022a) indicated that the maximum exceedance temperature of the fire in the bifurcation area was slightly higher than that of the fire located in the non-bifurcation area under longitudinal ventilation. Lu et al. (2022b) proposed an empirical model for the maximum ceiling temperature in the bifurcated tunnel under different fire locations with bifurcation angle between 20° and 90°. Li et al. (2021a, 2021b, 2021c) investigated the effects of transverse fire locations on the maximum exceedance temperature in a bifurcated tunnel fire. Chen et al. (2020a, 2020b) established a prediction model to predict the maximum exceedance temperature in a branched tunnel fire under natural ventilation, by considering the influence of ramp slopes.

However, there are few studies on the influence of ramp slopes on the maximum exceedance temperature under longitudinal ventilation in a branched tunnel. This research aims to quantify the combined effect of the ramp slope and longitudinal ventilation velocity on the maximum exceedance temperature beneath the ceiling in a branched tunnel fire. The results of this research could fill the research gap and provide a reference for the smoke exhaust design in branched tunnels.

2. Experiment system design and methods

A series of small-scale experiments were designed to investigate the influence of ramp slopes on the maximum exceedance temperature in a branched tunnel fire under longitudinal ventilation. The essential parameters of longitudinal ventilation velocities and ramp slopes were varied in a tunnel with a split angle of 15°.

A 1:20 scale-model bifurcated tunnel is established as shown in Fig. 1 to reflect the actual buoyancy-riven smoke movement induced by the fire through the results obtained from the small-scale experiments, the Froude similarity criterion (Li et al., 2019; Li et al., 2010; Quintiere, 1989) was adopted to design the model tunnel dimension and calculate the heat release rate and longitudinal ventilation velocity under experimental conditions. Based on the Froude similarity criterion, the temperature is the same between the model experiments and the actual

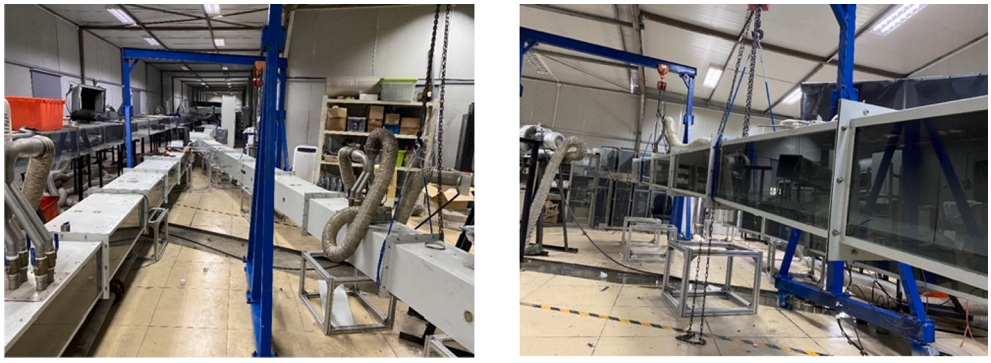

Fig. 1. Experiment setup.

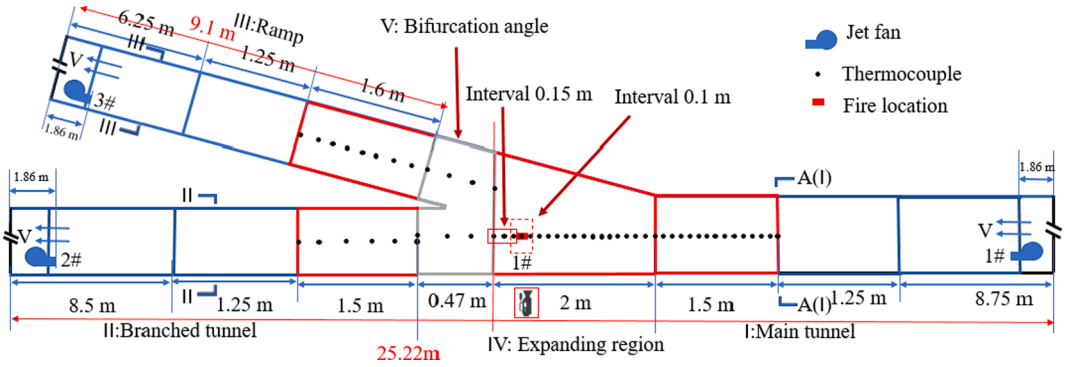

Fig. 2. The layout of the thermocouples (top view).

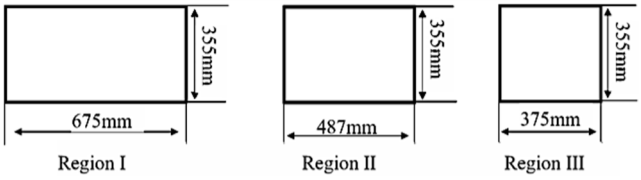

Fig. 3. The tunnel section.

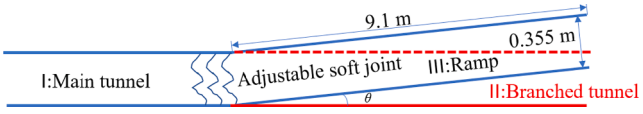

Fig. 4. The side view of the ramp, $\theta = 0$ %, 3 %, 5 %, 7 %, 9 %.

prototype scenarios, and the scaling models of the heat release rate and ventilation velocity between the model experiments and the actual prototype scenarios are deduced as follows:

$$Q_m/Q_f = \left(l_m/l_f\right)^{5/2} \tag{7}$$

$$V_m/V_f = \left(l_m/l_f\right)^{1/2} \tag{8}$$

As shown in Fig. 2, the model test bench consists of five parts, including the main tunnel before the bifurcation, the branch tunnel after the bifurcation, the ramp, the expanding region, and the bifurcation angle. The main tunnel is 25.22 m long and the ramp is 9.1 m long. Fig. 3 shows the schematic of the cross-sectional dimensions of the tunnel. The section dimension of the main tunnel before the expanding region is 0.675 m × 0.355 m. The section dimension of the branch tunnel after the bifurcation angle is 0.487 m × 0.355 m. The section dimensions of the ramp are 0.375 m × 0.355 m. Ramps and branching angles are combined by the adjustable soft joint, which is shown in Fig. 4. The gantry can change the slopes of the ramp within the range of 0 %−9 %.

The arrangement of the frequency conversion jet fans is shown in Fig. 2. Three groups of jet fans are hoisted 0.03 m beneath the ceiling along centre at the entrance of the main road tunnel. The diameter of the fans is 0.06 m. The distance between each group of jet fans is 0.07 m. The frequency conversion were used to provide longitudinal ventilation, which is uniformly distributed near the fire point.

The arrangement of K-type stainless steel-sheathed thermocouples with a diameter of 1.0 mm is shown in Fig. 2. The thermocouples were located 15 mm beneath the ceiling along the centreline of the tunnel (Gao et al., 2015; Ji et al., 2012; Huang et al., 2019; Huang et al., 2021). In the expending region, there are four groups of thermocouples, and each group of thermocouples includes four thermocouples along the centreline of the tunnel. The distance between the first three thermocouples is 0.15 m, and the distance between the fourth and the third is

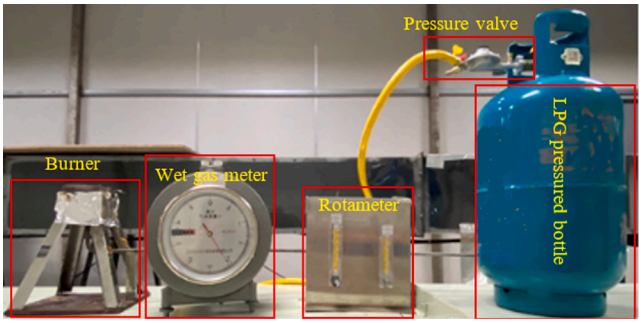

Fig. 5. The gas burner system.

0.05 m. The distance between each group of thermocouples is 0.05 m. Three sets of thermocouples are arranged within 1.5 m of the main tunnel away from the fire source, and the arrangement is the same as that in the expending region. Bifurcation Four thermocouples are evenly arranged with a spacing of 0.3 m in the bifurcation angle. Eight

Table 1
Experimental conditions.

No.	Heat release rate (kW)	Ventilation velocity (m/s)	ramp slope	fire location	Bifurcation angle (°)
A1	2.57	0, 0.52, 0.60, 0.66, 0.74	0 %	1#	15
A2	5.13	0, 0.77, 0.82, 0.86			
A3	7.70	0, 0.64, 0.83, 0.85, 0.93			
B1	2.57	0, 0.54, 0.65, 0.72	3 %		
B2	5.13	0, 0.72, 0.8, 0.85			
B3	7.70	0, 0.72, 0.85, 0.89			
C1	2.57	0, 0.64, 0.68, 0.78	5 %		
C2	5.13	0, 0.64, 0.70, 0.80			
C3	7.70	0, 0.70, 0.76, 0.87			
D1	2.57	0, 0.52, 0.60, 0.72	7 %		
D2	5.13	0, 0.68, 0.76, 0.80			
D3	7.70	0, 0.67, 0.74, 0.86			
E1	2.57	0, 0.55, 0.60, 0.67	9 %		
E2	5.13	0, 0.65, 0.77, 0.80			
E3	7.70	0, 0.71, 0.80, 0.83			

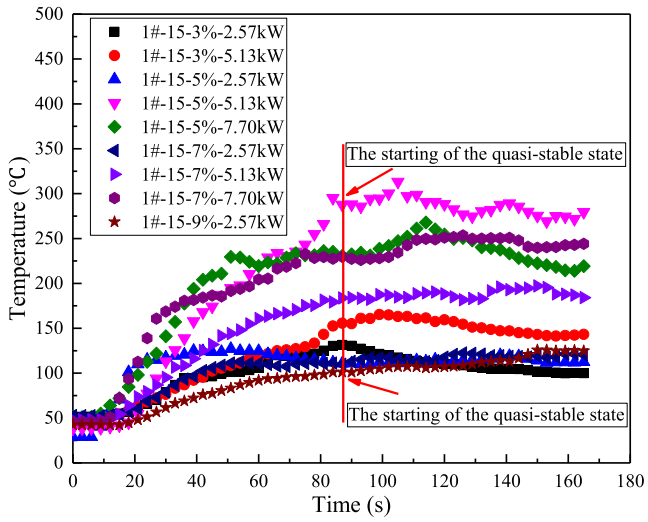

Fig. 6. The quasi-stable state of the experiments under natural ventilation.

thermocouples are evenly arranged within 1.6 m away from the fire source with a spacing of 0.2 m in the ramp tunnel. Five thermocouples are evenly arranged within 1.5 m away from the fire source with a spacing of 0.3 m in the branched tunnel.

The data collector Agilent 34972A was connected with the thermocouples to transform the measured signal to a PC. The fire-resistant glass thickness of 3 mm was inserted into one sidewall of the tunnel to provide a perspective to observe the shape of the fire plume and smoke movement characteristics. The rest of the tunnel wall is constructed of steel sheets with a thickness of 3 mm. A digital video and camera were adopted to record the shape of the fire plume and smoke movement characteristics.

The 1# fire point with dimensions of 100 mm × 100 mm × 100 mm was considered in this study located at the centre of the mainline away from the bifurcation angle of 0.3 m, shown in Fig. 2. Liquefied Petroleum Gas (LPG) was used as the fuel with an effective combustion heat of 43.7 MJ/kg (Oka et al., 2015; Li et al., 2021a, 2021b, 2021c). A pressure valve was used to turn on or off the fire system, and a rotameter was adopted to control the fuel flow rate. A wet gas metre with very few exceptions to about ± 1 % was adopted to measure the fuel flow rate. The entire fire source system is connected in series with five parts by pipes, as shown in Fig. 5.

The traffic flow is diverted from the main tunnel to the branch tunnel and ramp after the bifurcation, the jet fans was activated to supply longitudinal ventilation to the tunnel in case of fire. The longitudinal ventilation velocity at the A-A section was measured by a series of hot wire anemometers with a resolution of 0.01 m/s. Table 1 summarises all the experimental cases. The ramp of the prototype tunnel is 300 m × 7.5 m × 7.1 m. The branched tunnel of the prototype tunnel is 497 m × 9.74 m × 7.1 m. The main tunnel of the prototype tunnel is 703 m × 13.5 m × 7.1 m. Considering that the fire flame not impinging on the ceiling, the heat release rates of 2.57 kW, 5.13 kW and 7.70 kW were used to analyze the maximum exceedance temperature, conversion to full-scale heat release rates of 4.6 MW, 9.2 MW and 13.8 MW. Considering the difference of the velocity in the branch tunnel, ramp and main tunnel, the critical longitudinal ventilation velocity was defined as the velocity in the main tunnel when the smoke back-layering length was 0 m for current experimental study. The longitudinal ventilation velocity ranges from 0 m/s to the critical longitudinal ventilation velocity (m/s) to analyze the influence of the longitudinal ventilation on the maximum exceedance temperature.

3. Results and discussion

According to the previous studies (Huang et al., 2019; Lei et al., 2022), the maximum exceedance temperature model under nature ventilation is similar to the maximum exceedance temperature model under dimensionless velocity less than 0.19. The influence of low longitudinal ventilation velocity on maximum exceedance temperature is weak. And even this influence could be ignored when the heat release rate is relatively high. Therefore, the maximum exceedance temperature model is divided into two parts by normalized ventilation velocity 0.19.

3.1. Maximum exceedance temperature under small ventilation with $V' < 0.19$

Fig. 6 shows the temperature change with the time beneath the ceiling at the fire location under natural ventilation. It indicates that the temperature begin to increase and then remains quasi-stable within small floating, when the burn time reaches 80 s under natural ventilation. This is because the combustion of the LPG keeps the quasi-stable state heat release rate. He et al. (2021) indicated that the qualitative analysis about the fire flame characteristics could be observed by typical pictures at quasi-stable moments.

Fig. 7 presents the shape of the fire plume in the tunnel with different heat release rates and ramp slopes under natural ventilation. Fig. 7(a) and Fig. 7(b) illustrate that the fire plume tends to be vertical when the ramp slope is 0 % and 3 %. When the ramp slope is 0 %, the entrainment induced by the stack effect is weaker than the entrainment induced by the fire plume buoyancy.

Fig. 7(c) displays the shape of the fire plume when the ramp slope is 5 %. For a given the heat release rate of 2.57 kW, the fire plume tilts to the side of the bifurcation angle. When the heat release rate is 2.57 kW, the entrainment induced by the fire plume buoyancy is weaker than the entrainment induced by the stack effect. The entrainment is asymmetrically at the two sides of the fire plume, causing the fire plume to tilt towards the branch. The fire plume tends to be vertical when the heat release rate reaches 5.13 kW. Fig. 7(d) and Fig. 7(e) displays the shape of the fire plume when the ramp slopes are 7 % and 9 %, respectively. There are similar changes in the shape of the flame when the ramp slopes vary from 5 % to 9 %.

For a given the heat release rate of 2.57 kW, the inclination angle of the fire plume increases as the ramp slope increases by comparing the result of different ramp slopes. The entrainment induced by the stack effect increases as the ramp slope increases. The fire plume tends to be vertical when the heat release rate reaches 5.13 kW with different ramp slopes. The main reason could be that the entrainment induced by the stack effect is weaker than the entrainment induced by the fire plume buoyancy. The fire plume is influenced by both the ramp slopes and the heat release rates.

Fig. 8 indicates the comparisons between the experimental data and those results predicted by previous maximum exceedance temperature models (Hu et al., 2013; Huang et al., 2019; Chen et al., 2020a, 2020b). Hu et al. (2013) carried out a series of small-scale experiments to investigate the influence of the tunnel slopes on the maximum exceedance temperature. The maximum exceedance temperature predicted by the model (Hu et al., 2013) is the lowest among the results because the experiment was carried out in an inclined tunnel. Under fire, the stack effect induced by a tilted tunnel is stronger than that of the branched tunnel with the tilted ramp. The stack effect not only accelerates the entrainment of air but also accelerates the smoke flow velocity. From Fig. 8, the maximum temperature predicted by the model (Chen et al., 2020) is higher than the experiment results and other calculated values. The reason is that the fire plume impinges on the ceiling in the experiment. Due to the limitation of the sidewalls and the ceiling, combustion of fuel and air entrainment would be greatly limited because of the fire plume impinging on the tunnel ceiling and spreading to both sides of the ceiling. The experimental results and Huang's model is similar under a

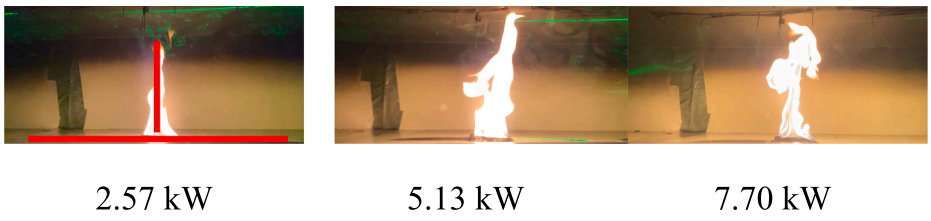

2.57 kW 5.13 kW 7.70 kW

(a) The ramp slope of 0%.

2.57 kW 5.13 kW 7.70 kW

(b) The ramp slope of 3%.

2.57 kW 5.13 kW 7.70 kW

(c) The ramp slope of 5%.

2.57 kW 5.13 kW 7.70 kW

(d) The ramp slope of 7%.

2.57 kW 5.13 kW 7.70 kW

(e) The ramp slope of 9%.

Fig. 7. The flame plume under natural ventilation.

ramp slope of 0 %. Thus, a new correlation to illustrate the influence of the ramp slopes on the maximum exceedance temperature in a branched tunnel fire is essential to be established.

According to the experimental results in Fig. 8, the influence of ramp slopes on the maximum exceedance temperature is not significant for a given small heat release rate compared with the large heat emission rate. The difference in the maximum excessed temperature becomes larger with the ramp slope increasing compared to the maximum excessed temperature with a ramp slope of 0 % under a large heat release rate, due to results from the stack effect becoming stronger with increasing heat release rate in an inclined tunnel fire (Zhang et al., 2021a, 2021b, 2021c; Du et al., 2018; Chow et al., 2016). Also, the stack effect is taken away the heat. However, the stack effect accelerates the entrainment of cool air into the smoke layer and fire plume, which enhances the

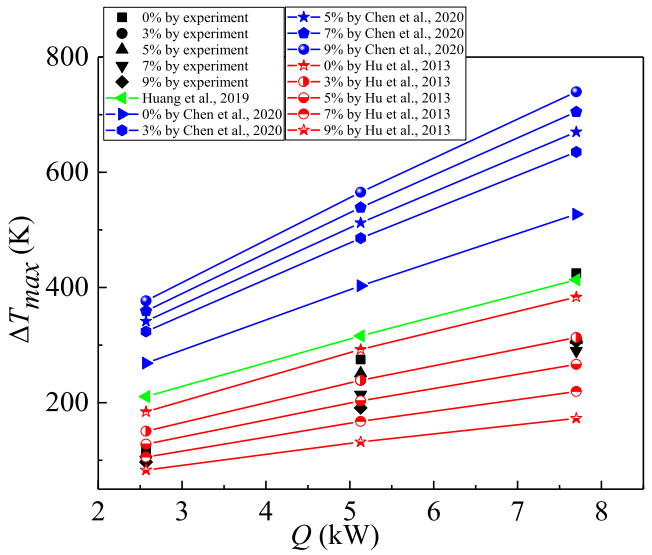

Fig. 8. A comparison of experimental results with previous studies.

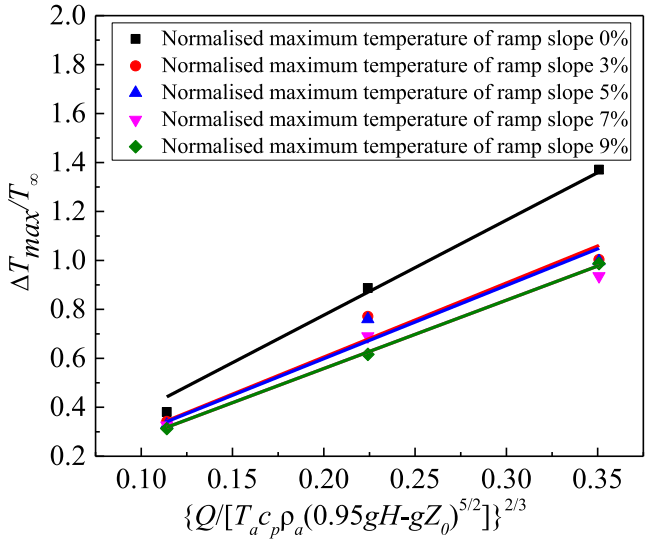

Fig. 9. The relationship between normalised maximum temperatures with normalised HRR.

convection heat transfer.

Fig. 9 illuminates the relationship between the normalised maximum temperature excess and the normalised heat emission rate. The normalised maximum temperature excess varies as 2/3 power of the normalised heat release rate for a given split angle. Thus, the 2/3 power of the normalised heat release rate was selected as the normalised parameter to analyze the influence of the ramp slopes on the normalised maximum temperature excess. A coefficient α_θ is put forward to modify the influence of the ramp slopes on the maximum exceedance temperature according to the model (Huang et al., 2019). According to the previous studies (Huang et al., 2019; Lei et al., 2022), the linear correlation illustrates well the relationship between the normalised maximum temperature and normalised heat release rate. The modified model could be expressed as follows in Eq. (9):

$$\frac{\Delta T_{\max}}{T_\infty} = \alpha_\theta \left(\frac{Q}{T_\infty c_p \rho_\infty \sqrt{g(0.95H - Z_0)^5}} \right)^{2/3} \tag{9}$$

For a given ramp slope, the fitted value between the dimensionless maximum temperature excess and the different dimensionless parameter is summarised in Table 2. Fig. 10 plots the correlation of the fitted value of α_θ with ramp slopes. The effect of the slopes has a linear relationship with the maximum exceedance temperature. The linear relationship of the effect of slopes with the maximum exceedance temperature could be expressed as follows:

$$\alpha_\theta = -0.065\theta + 3.296 \tag{10}$$

Taking Eq. (10) into Eq. (9), the maximum exceedance temperature beneath the tunnel ceiling could be predicted by the empirical formula under natural ventilation.

Table 2
The fitting value of the variables, α_θ.

Item	Values				
Ramp slopes	0 %	3 %	5 %	7 %	9 %
α_θ	3.35	3.02	2.99	2.79	2.76

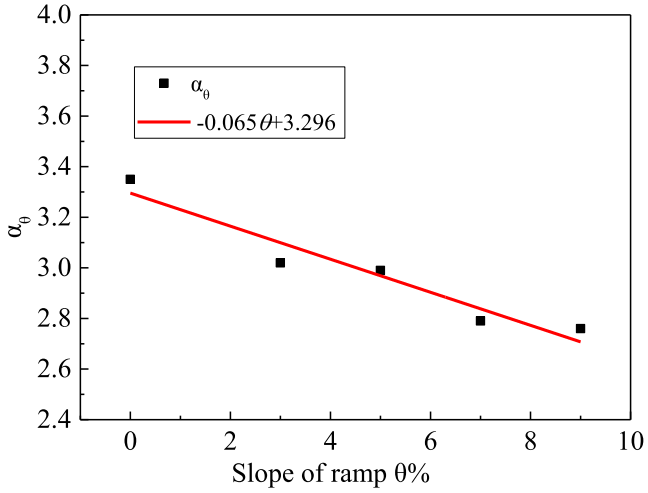

Fig. 10. The correlation of the fitted value of α_θ with ramp slopes.

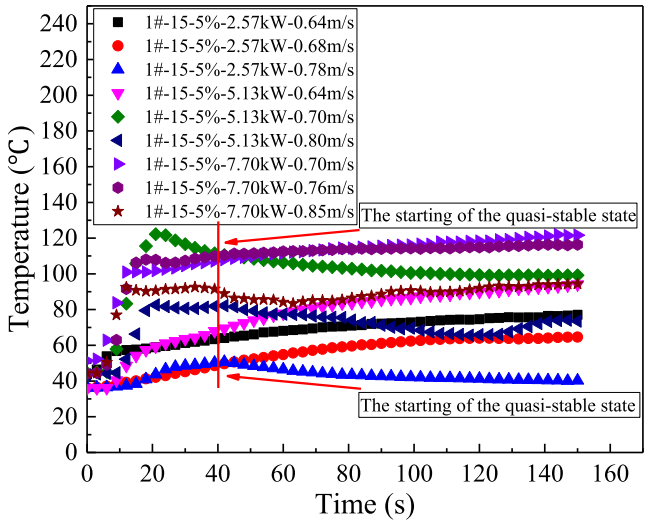

Fig. 11. The quasi-stable state of the experiments under longitudinal ventilation.

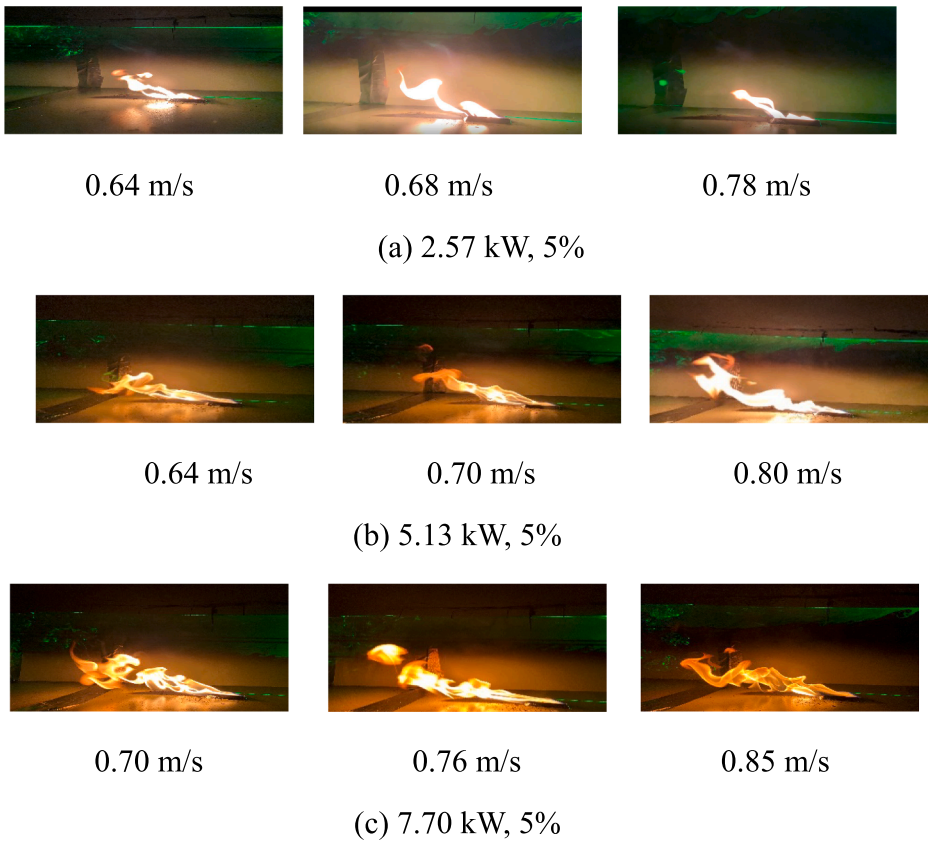

Fig. 12. The flame plume under longitudinal ventilation with the ramp slope of 5%.

3.2. Maximum temperature excess under longitudinal ventilation with V'>0.19

Fig. 11 shows the temperature change with the time beneath the ceiling at the fire location under longitudinal ventilation. It indicates that the temperature begin to increase and then remains quasi-stable state within small floating, when the burn time reaches 40 s under longitudinal ventilation. The experimental results reveal that the heat release rate and longitudinal ventilation remains quasi-stable in the tunnel. Otherwise, the temperature would change continuously.

Fig. 12 presents the shape of the fire plume in the tunnel with ramp slope of 5 % under different heat release rates and longitudinal ventilation. The fire flame was tilted to the downstream and the fire flame was beneath the tunnel ceiling. Fig. 12(a) demonstrates that small longitudinal ventilation velocity is conducive to the combustion of the fire source because of more oxygen supplied to the fire source. However, a large longitudinal ventilation velocity suppresses the combustion of the fire source because of more heat of combustion loss caused by the longitudinal ventilation.

Fig. 12(b) points out that the combustion of the fire became more with the increase in the longitudinal ventilation velocity. This is because the oxygen supply effect caused by the longitudinal ventilation was greater than the cooling suppression influence of the longitudinal ventilation.

Fig. 12(c) denotes that the ventilation effect has little effect on the combustion of the fire, and the shape of the fire plume remains stable under different longitudinal ventilation velocities. The fire plume pattern remained continuous among the different heat release rates when the longitudinal ventilation velocity was less than the critical longitudinal ventilation velocity.

The effect of the ramp slope on the smoke spread is due to the formation of the stack effect. When the longitudinal ventilation and the stack effect are coupled to affect the smoke spread, the effect of

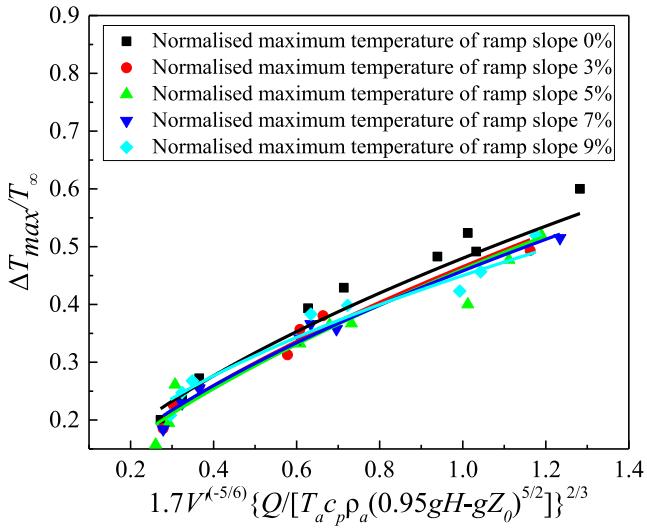

Fig. 13. The relationship between normalised maximum temperatures with normalised parameters.

Table 3
The fitting values of the coefficient ξ and power φ.

Item	Values				
Ramp slopes	0 %	3 %	5 %	7 %	9 %
ξ	0.480	0.465	0.461	0.458	0.450
φ	0.601	0.637	0.650	0.619	0.531

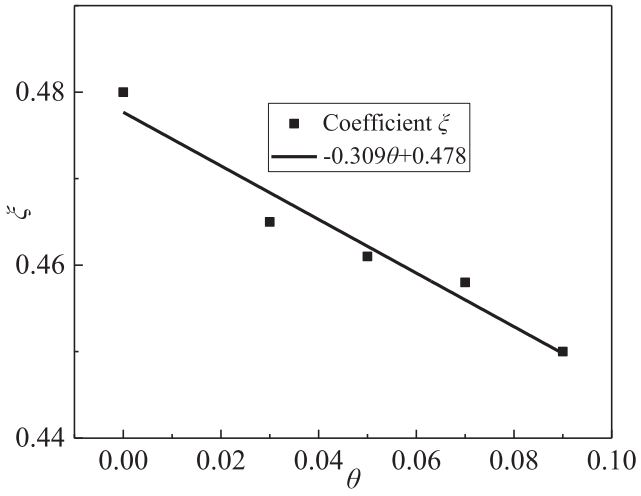

(a) Relationship of coefficient ξ with ramp slope θ.

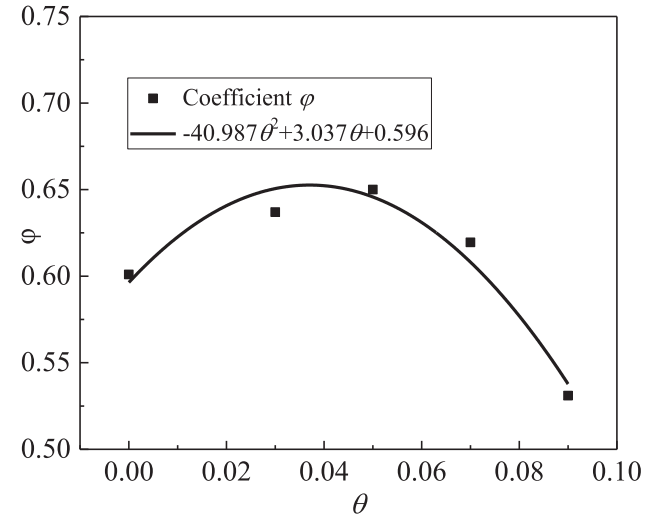

(b) Relationship of coefficient φ with ramp slope θ.

Fig. 14. The relationship of coefficients with a ramp slope for normalised maximum temperatures.

longitudinal ventilation is dominant.

Fig. 13 points out the relationship between the normalised maximum temperature excess and the normalised parameter. The normalised maximum temperature excess fits well with the normalised parameter by the exponential relationship according to Eq. (11) under $V' > 0.19$. The exponential coefficients are different from the ramp slopes. The fitting values of the coefficient ξ and power φ are summarised in Table 3.

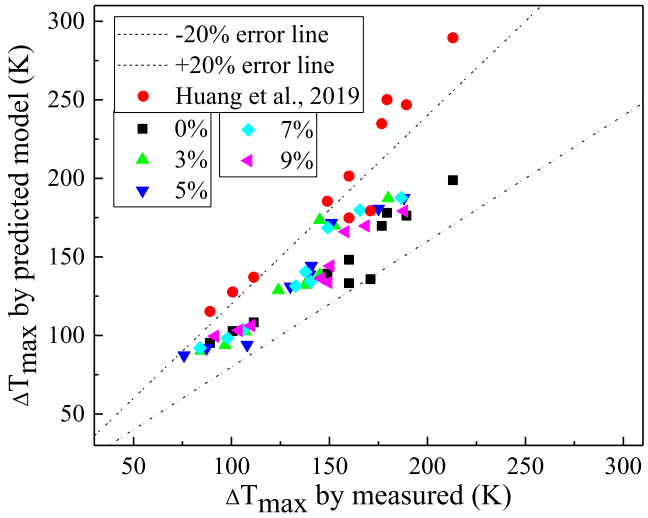

Fig. 15. The comparison of the maximum exceedance temperature among the predicted model, experimental results, and previous model.

$$\frac{\Delta T_{max}}{T_\infty} = \xi\left\{1.7V^{-5/6}\left(\frac{Q}{T_\infty c_p \rho_\infty \sqrt{g(0.95H - Z_0)^5}}\right)^{2/3}\right\}^{\varphi} \tag{11}$$

$$\begin{cases} \xi = -0.309\theta + 0.478 \\ \varphi = -40.987\theta^2 + 3.037\theta + 0.596 \end{cases} \tag{12}$$

Fig. 14 denotes the correlation between the coefficients and the ramp slopes. The correlation could be described by Eq. (12). Substituting Eq. (12) into Eq. (11), the maximum exceedance temperature could be predicted by the empirical formula under longitudinal ventilation.

Fig. 15 shows the comparison of maximum temperature excess predicted by Eq. (11) and Eq. (12) with experimental results and a previous prediction model proposed by Huang (Huang et al., 2019). The maximum exceedance temperature is predicted by Eq. (11) and Eq. (12) are consistent with the experimental results. The calculated values by the previous model (Huang et al., 2019) are larger than the experimental results owing to the applicability of Huang's model for the horizontal branched tunnel fire.

By considering the effect of the ramp slope, the prediction model of maximum temperature excess is modified according to the experimental results. The prediction model of maximum temperature excess beneath the tunnel ceiling in a branched tunnel with the inclined ramp could be derived into two parts (V, V) as Eq. (13).

$$\frac{\Delta T_{max}}{T_\infty} = \begin{cases} (-0.65\theta + 3.296)\left(\dfrac{Q}{T_\infty c_p \rho_\infty \sqrt{g(0.95H - Z_0)^5}}\right)^{2/3}, & V' < 0.19 \\ (-0.309\theta + 0.478)\left\{1.7V^{-5/6}\left(\dfrac{Q}{T_\infty c_p \rho_\infty \sqrt{g(0.95H - Z_0)^5}}\right)^{2/3}\right\}^{\left(-40.987\theta^2 + 3.037\theta + 0.596\right)}, & V' \geqslant 0.19 \end{cases} \tag{13}$$

4. Conclusion

In this study, systematic experiments were conducted to investigate the maximum exceedance temperature beneath the tunnel ceiling in a

reduced scale branched tunnel under longitudinal ventilation with different ramp slopes. A model of the maximum exceedance temperature was established for the bifurcated tunnel fire. The major conclusions are as follows:

(1) Under the natural ventilation, for a branched tunnel with the bifurcation angle of 15°, the influence of ramp slopes (0 % − 9 %) on the fire plume is relatively significant with a small heat release rate under the natural ventilation. The incline of the fire plume is more obvious for the experiments with larger ramp slopes. When the longitudinal ventilation and the stack effect are coupled to affect the smoke spread, the effect of longitudinal ventilation is dominant.
(2) Under the natural ventilation, the maximum exceedance temperature beneath the ceiling decreases with an increase in the ramp slope under the natural ventilation in the main tunnel. The cooling effect of the stack effect induced in the ramp is larger than the oxygen supply effect caused by the entrainment. Under the longitudinal ventilation, the maximum exceedance temperature beneath the ceiling decreases with an increase in the ramp slope under the longitudinal ventilation in the main tunnel.
(3) The modified correlation of the maximum exceedance temperature has been established by considering the ramp slopes under the different ventilation with the bifurcation angle of 15°.

This article proposes new correlations for the calculation of the maximum gas excess temperature beneath the ceiling in a branched tunnel. However, the temperature profile inside the tunnel is also dependent on compositive effect of multiple factors, such as the bifurcation angles, sealing rates, which should be investigated further. For full-scale fires, due to the different structure properties and boundary conditions, the radiation may be more complex. The correlations developed from small-scale experiments might have limitations while they are extended to full-scale cases as the radiation is not scaled similarly as the convection. More experiments of different scales, higher heat release rates and numerical CFD simulations would be useful to provide more insights, and to further explore the application of findings in the present study as a potential future work.

CRediT authorship contribution statement

Jiaxin Li: Conceptualization, Data curation, Formal analysis, Methodology, Writing – original draft. **Yanfeng Li:** Project administration, Supervision, Writing – review & editing. **Junmei Li:** Funding acquisition, Writing – review & editing. **Hua Zhong:** Writing – review & editing. **Jianlong Zhao:** Investigation, Data curation. **Desheng Xu:** Investigation, Data curation.

Declaration of Competing Interest

The authors declare that they have no known competing financial interests or personal relationships that could have appeared to influence the work reported in this paper.

Data availability

The data that has been used is confidential.

Acknowledgements

This study was funded by the Beijing Natural Science Foundation (Grant No: 8222002) and the project of China Scholarship Council (CSC, Grant No. 202206540054).

References

Alpert, R.L., 1972. Calculation of response time of ceiling-mounted fire detectors. Fire Technol. 8, 181–195.
Chen, L.F., Mao, P.F., Zhang, Y.Z., Xing, S.S., Li, T., 2020a. Experimental study on smoke characteristics of bifurcated tunnel fire. Tunn. Undergr. Space Technol. 98, 103295.
Chen, C.K., Nie, Y.L., Zhang, Y.L., Lei, P., Fan, C.G., Wang, Z.Y., 2020b. Experimental investigation on the influence of ramp slope on fire behaviors in a bifurcated tunnel. Tunn. Undergr. Space Technol. 104, 103522.
Chow, W.K., Gao, Y., Zhao, J.H., Dang, J.F., Chow, C.L., Miao, L., 2015. Smoke movement in tilted tunnel fires with longitudinal ventilation. Fire Saf. J. 75, 14–22.
Chow, W.K., Gao, Y., Zhao, J.H., Dang, J.F., Chow, C.L., 2016. A study on tilted tunnel fire under natural ventilation. Fire Saf. J. 81, 44–57.
Du, T., Yang, D., Ding, Y., 2018. Driving force for preventing smoke backlayering in downhill tunnel fires using forced longitudinal ventilation. Tunn. Undergr. Space Technol. 79, 76–82.
Gannouni, S., 2022. Critical velocity for preventing thermal backlayering flow in tunnel fire using longitudinal ventilation system: effect of floor-fire separation distance. Int. J. Therm. Sci. 171, 107192.
Gao, Z.H., Ji, J., Fan, C.G., Sun, J.H., 2015. Experimental analysis of the influence of accumulated upper hot layer on the maximum ceiling gas temperature by a modified virtual source origin concept. Int. J. Heat Mass Tran. 84, 262–270.
He, K., Cheng, X.D., Li, Y.Z., Ingason, H., Shi, Z.C., Yang, H., Zhang, H.P., 2021. Experimental study on flame characteristics of double fires in a naturally ventilated tunnel: Flame merging, flame tilt angle and flame height. Tunn. Undergr. Space Technol. 114, 103912.
Heskestad, G., 1983. Luminous heights of turbulent diffusion flames. Fire Saf. J. 5 (2), 103–108.
Hu, L.H., Chen, L.F., Wu, L., Li, Y.F., Zhang, J.Y., Meng, N., 2013. An experimental investigation and correlation on buoyant gas temperature below ceiling in a slopping tunnel fire. Appl. Therm. Eng. 51, 246–254.
Huang, Y.B., Li, Y.F., Li, J.M., Li, J.X., Wu, K., Zhu, K., Li, H.H., 2019. Experimental investigation on maximum gas temperature beneath the ceiling in a branched tunnel fire. Int. J. Therm. Sci. 145, 105997.
Huang, Y.B., Li, Y.F., Li, J.M., Li, J.X., Wu, K., Zhu, K., Li, H.H., 2020. Modelling and experimental investigation of critical velocity and driving force for preventing smoke backlayering in a branched tunnel fire. Tunn. Undergr. Space Technol. 99, 103388.
Huang, Y.B., Li, Y.F., Li, J.X., Wu, K., Li, H.H., Zhu, K., 2021. Experimental study on the temperature longitudinal distribution induced by a branched tunnel fire. Int. J. Therm. Sci. 170, 107175.
Huang, Y.B., Li, Y.F., Li, J.X., Wu, K., Li, H.H., Zhu, K., Li, J.M., 2022. Experimental investigation of the thermal back-layering length in a branched tunnel fire under longitudinal ventilation. Int. J. Therm. Sci. 173, 107415.
Ingason, H., Lönnermark, A., 2005. Heat release rates from heavy goods vehicle trailer fires in tunnels. Fire Saf. J. 40, 646–668.
Ji, J., Fan, C.G., Zhong, W., Shen, X.B., Sun, J.H., 2012. Experimental investigation on influence of different transverse fire locations on maximum smoke temperature under the tunnel ceiling. Int. J. Heat Mass Tran. 55, 4817–4826.
Kong, J., Xu, Z.S., You, W.J., Wang, B.L., Liang, Y., Chen, T., 2021. Study of smoke back-layering length with different longitudinal fire locations in inclined tunnels under natural ventilation. Tunn. Undergr. Space Technol. 107, 103663.
Lei, P., Chen, C.K., Zhang, Y.L., Xu, T., Sun, H.K., 2021. Experimental study on temperature profile in a branched tunnel fire under natural ventilation considering different fire locations. Int. J. Therm. Sci. 159, 106631.
Lei, P., Chen, C.K., Zhao, D.Y., Zhang, Y.L., Xu, T., Jiao, W.B., 2022. Study on heat allocation and temperature profile in a T-shaped branched tunnel fire with different branch slopes under natural ventilation. Tunn. Undergr. Space Technol. 126, 104508.
Li, Z.S., Gao, Y.J., Li, X.S., Mao, P.F., Zhang, Y.C., Jin, K.Y., Li, T., Chen, L.F., 2021b. Effects of transverse fire locations on flame length and temperature distribution in a bifurcated tunnel fire. Tunn. Undergr. Space Technol. 112, 103893.
Li, Y.Z., Lei, B., Ingason, H., 2010. Study of critical velocity and backlayering length in longitudinally ventilated tunnel fires. Fire Saf. J. 45, 361–370.
Li, Y.Z., Lei, B., Ingason, H., 2011. The maximum temperature of buoyancy-driven smoke flow beneath the ceiling in tunnel fires, Fire Saf. J. 46, 204–210.
Li, J., Li, Y.F., Cheng, C.H., Chow, W.K., 2019. A study on the effects of the slope on the critical velocity for longitudinal ventilation in tilted tunnels. Tunn. Undergr. Space Technol. 89, 262–267.
Li, J.X., Li, Y.F., Li, J.M., Li, X.J., Huang, Y.B., 2021c. Study on smoke control under mechanical exhaust strategy in a cross-type interchange subway station. Tunn. Undergr. Space Technol. 112, 103897.
Li, H.H., Tang, F., 2022. Numerical and experimental study on the critical velocity and smoke maximum temperature in the connected area of branch tunnel. Build Simul-China. 15, 525–536.
Li, Y.S., Zhang, X.L., Sun, X.P., Zhu, N., 2021a. Maximum temperature of ceiling jet flow in longitudinal ventilated tunnel fires with various distances between fire source and cross-passage. Tunn. Undergr. Space Technol. 113, 103953.
Lu, X.L., Weng, M.C., Liu, F., Wang, F., Han, J.Q., Cheung, S.C., 2022a. Study on smoke temperature profile in bifurcated tunnel fires with various bifurcation angles under natural ventilation. J. Wind Eng. Ind. Aerod. 225, 105001.
Lu, X.L., Weng, M.C., Liu, F., Wang, F., Han, J.Q., Cheung, S.C., 2022b. Effect of bifurcation angle and fire location on smoke temperature profile in longitudinal ventilated bifurcated tunnel fires. Tunn. Undergr. Space Technol. 127, 104610.
McCaffrey, B., 1979. Purely Buoyant Diffusion Flames. Washington DC: National Bureau of Standards.

Oka, Y., Oka, H., Imazeki, O., 2015. Temperature distribution within a ceiling jet propagating in an inclined flat-ceilinged tunnel with natural ventilation. Fire Saf. J. 71, 68–77.
Quintiere, J.G., 1989. Scaling applications in fire research. Fire Saf. J. 15, 3–29.
Tanaka, F., Yoshida, K., Ueda, K., Ji, J., 2021. A simple model for predicting the smoke spread length during a fire in a shallow urban road tunnel with roof openings under natural ventilation. Fire Saf. J. 120, 103106.
Tomar, M.S., Khurana, S., 2019. Impact of passive fire protection on heat release rates in road tunnel fire: A review. Tunn. Undergr. Space Technol. 85, 149–159.
Wang, J., Fan, Y.J., Wei, Y.Q., Jiang, X.P., Lu, K.H., 2021. Effect of the blockage ratio on the smoke extraction efficiency in tunnel fires with natural ventilation. Tunn. Undergr. Space Technol. 117, 104165.
Wang, F., Wang, M.N., 2016. A computational study on effects of fire location on smoke movement in a road tunnel. Tunn. Undergr. Space Technol. 51, 405–413.
Zhang, X.L., Lin, Y.J., Shi, C.L., Zhang, J.P., 2021c. Numerical simulation on the maximum temperature and smoke back-layering length in a tilted tunnel under natural ventilation. Tunn. Undergr. Space Technol. 107, 103661.
Zhang, T.H., Wang, G.Y., Hu, H.H., Huang, Y.D., Zhu, K., Wu, K., 2021a. Study on temperature decay characteristics of fire smoke backflow layer in tunnels with wide-shallow cross-section. Tunn. Undergr. Space Technol. 112, 103874.
Zhang, X.C., Zhang, Z.Y., Tao, H.W., 2021b. A numerical study on critical velocity and back-layering length with trains' blockage in longitudinally ventilated tunnel fires. Tunn. Undergr. Space Technol. 116, 104093.
Zhou, Y., Chen, F., Geng, Z.Y., Bu, R.G., Gong, W.X., Fan, C.G., Yi, L., 2021. Experimental study on the characteristics of temperature distribution of two pool fires with different transverse locations in a naturally ventilated tunnel. Tunn. Undergr. Space Technol. 116, 104095.
Zukoski, E.E., Kubota, T., Cetegen, B., 1981. Entrainment in fire plumes. Fire Saf. J. 3, 107–121.